

Linköping University Post Print

EGR-VGT Control and Tuning for Pumping Work Minimization and Emission Control

Johan Wahlström, Lars Eriksson and Lars Nielsen

N.B.: When citing this work, cite the original article.

©2009 IEEE. Personal use of this material is permitted. However, permission to reprint/republish this material for advertising or promotional purposes or for creating new collective works for resale or redistribution to servers or lists, or to reuse any copyrighted component of this work in other works must be obtained from the IEEE.

Johan Wahlström, Lars Eriksson and Lars Nielsen, EGR-VGT Control and Tuning for Pumping Work Minimization and Emission Control, 2010, IEEE Transactions on Control Systems Technology, (18), 4, 993-1003.

<http://dx.doi.org/10.1109/TCST.2009.2031473>

Postprint available at: Linköping University Electronic Press

<http://urn.kb.se/resolve?urn=urn:nbn:se:liu:diva-18336>

EGR-VGT Control and Tuning for Pumping Work Minimization and Emission Control

Johan Wahlström, Lars Eriksson, and Lars Nielsen

Abstract—A control structure is proposed and investigated for coordinated control of exhaust gas recirculation (EGR) valve and variable geometry turbochargers (VGT) position in heavy duty diesel engines. Main control goals are to fulfill the legislated emission levels, to reduce the fuel consumption, and to fulfill safe operation of the turbocharger. These goals are achieved through regulation of normalized oxygen/fuel ratio, λ_O , and intake manifold EGR-fraction. These are chosen both as main performance variables and feedback variables since they contain information about when it is possible to decrease the fuel consumption by minimizing the pumping work. Based on this a novel and simple pumping work minimization strategy is developed. The proposed performance variables are also strongly coupled to the emissions which makes it easier to adjust set-points, e.g., depending on measured emissions during an emission calibration process, since it is more straightforward than control of manifold pressure and air mass flow. Further, internally the controller is structured to handle the different control objectives. Controller tuning is important for performance but can be time consuming so the controller objectives are captured in a cost function, which makes automatic tuning possible even though objectives are conflicting. Performance tradeoffs are necessary and are illustrated on the European Transient Cycle. The controller is validated in an engine test cell, where it is experimentally demonstrated that the controller achieves all the control objectives and that the current production controller has at least 26% higher pumping losses compared to the proposed controller.

Index Terms—Diesel engine modeling, exhaust gas recirculation (EGR)-fraction, engine control, oxygen/fuel ratio, proportional-integral-derivative (PID).

I. INTRODUCTION

LEGISLATED emission limits for heavy duty trucks are constantly reduced while at the same time there is a significant drive for good fuel economy. To fulfill the requirements, technologies like exhaust gas recirculation (EGR) systems and variable geometry turbochargers (VGT) have been introduced. The primary emission reduction mechanisms utilized are that NO_x can be reduced by increasing the intake manifold EGR-fraction and smoke can be reduced by increasing the air/fuel ratio [1]. However the EGR fraction and air/fuel ratio depend in complicated ways on the EGR and VGT actuation and it is therefore necessary to have coordinated control of the EGR and VGT to reach the legislated emission limits. Various approaches have been published, and an overview of different control aspects is

given in [2]. A multi-variable controller is presented in [3], some approaches that differ in the selection of performance variables are compared in [4], and in [5] decoupling control is investigated. Other control approaches are described in [6]–[12].

This paper presents the scientifically interesting results from an academic and industrial collaboration where a structure for coordinated EGR and VGT control was developed and investigated. The structure provides a convenient way for handling emission requirements and introduces a novel and straightforward approach for optimizing the engine efficiency by minimizing pumping work. Added to that, the paper covers requirements regarding additional control objectives, interfaces between inner and outer loops, and calibration that have been important for a successful industrial validation and application. The paper includes modeling, system analysis, systematic control design, tuning, simulations, and experimental validations.

II. PROPOSED CONTROL APPROACH

To deliver low fuel consumption and fast response to the driver's command while fulfilling the emission requirements are the goals for engine control. The control of EGR and VGT for emission abatement is considered first, and then the other goals are considered as they are also important for a successful application. The selection of performance and feedback variables is an important first step [13], and for emission control it should be noted that exhaust gases, present in the intake from EGR, also contain oxygen. This makes it more suitable to define and use the oxygen/fuel ratio instead of the traditional air/fuel ratio. The main motive is that it is the oxygen content that is crucial for smoke generation, and the idea is to use the oxygen content of the cylinder instead of air mass flow, see, e.g., [14]. The exact definition of the normalized oxygen/fuel ratio λ_O is given by (16) in Section III. Thus, EGR-fraction x_{egr} and oxygen/fuel ratio λ_O are a natural selection for performance variables as they are directly related to the emissions. These performance variables are equivalent to cylinder air/fuel ratio and burned gas ratio which are a frequent choice for performance variables in many papers [3], [4], [11], [12].

The choice of feedback variables defines the overall controller structure, and the most common choice in the literature are compressor air mass flow and intake manifold pressure [4], [5], [9], [10], [12]. Other choices are intake manifold pressure and EGR-fraction [4], exhaust manifold pressure and compressor air mass flow [3], intake manifold pressure and EGR flow [15], intake manifold pressure and cylinder air mass-flow [6], or compressor air mass flow and EGR flow [8]. Based on the close relation to the emissions, x_{egr} and λ_O are here used also as feedback variables. Simulations are presented in [11], but to our knowledge our work is the first that have utilized and verified this choice of feedback variables experimentally.

Manuscript received April 27, 2008; accepted August 12, 2009. Manuscript received in final form August 26, 2009. First published October 09, 2009; current version published June 23, 2010. Recommended by Associate Editor C. Bohn. This work was supported by the Swedish Energy Agency and Scania CV AB.

The authors are with the Vehicular Systems, Electrical Engineering, Linköping University, Linköping 58183, Sweden (e-mail: johwa@isy.liu.se; larser@isy.liu.se; lars@isy.liu.se).

Digital Object Identifier 10.1109/TCST.2009.2031473

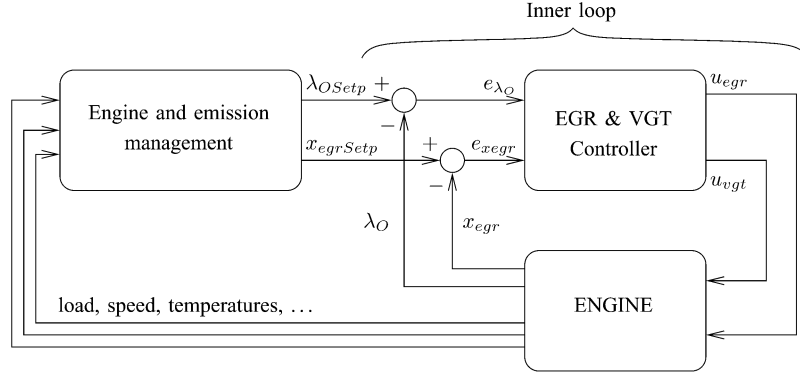


Fig. 1. Cascade control structure, with an inner loop where EGR and VGT actuators are controlled using the main performance variables EGR fraction x_{egr} and oxygen/fuel ratio λ_O . This sketch is a simplified illustration of the main idea that will be completed in Section V to also include fuel control and turbo protection.

A. Advantages of This Choice

There are three main advantages with the choice of EGR-fraction x_{egr} and oxygen/fuel ratio λ_O as both performance and feedback variables.

The first advantage is that these variables provide direct information about when it is possible/allowed to minimize the pumping work, compared to, e.g., manifold pressure and air mass flow. To facilitate improved fuel economy the proposed control structure also has a novel and simple mechanism for optimizing the fuel consumption by minimizing the pumping work. In diesel engines a large λ_O is allowed and there is thus an extra degree of freedom, when λ_O is greater than its set-point, that can be used to minimize the pumping work. Pumping minimization is an important feature, however the performance variables x_{egr} and λ_O are always controlled as they are the major variables in the controller.

The second advantage is as mentioned above that these variables are strongly connected to the emissions and gives a natural separation within the engine management system. The performance variables are handled in a fast inner loop, whereas trade-offs between, e.g., emissions and response time for different operating conditions are made in an outer loop. The idea with two loops is depicted in Fig. 1.

The third follows from the second in that it fits well into industry's engineering process where the inner control loops are first tuned for performance. Then the total system is calibrated to get stable combustion and to meet the emission limits by adjusting set-points for different operating conditions, different hardware configurations, and different legislative requirements depending on the measured emissions during the emission calibration process.

Normally, neither x_{egr} nor λ_O are measured and have to be estimated using observers. The observer design is important, but it is not the focus in this paper. Here it is assumed that an observer exist similar to that in [11]. This means that the known issues about oxygen estimation are handled and in the experiments such an observer of industrial production type is available and used. Engines could in the future be equipped with a sensor for λ_O , and if so, then nothing has to be changed in the proposed controller structure, which is an additional advantage.

B. Control Objectives

In addition to control of x_{egr} and λ_O it is also necessary to have load control, since the driver's demand must be actuated. This is achieved through basic fuel control using feedforward. Furthermore it is also important to monitor and control turbocharger speed since aggressive transients can cause damage through over-speeding.

The primary variables to be controlled are engine torque M_e , normalized oxygen/fuel ratio λ_O , intake manifold EGR-fraction x_{egr} , and turbocharger speed n_t . The goal is to follow a driving cycle while maintaining low emissions, low fuel consumption, and suitable turbocharger speeds, which together with the discussion above gives the following control objectives for the performance variables.

- 1) λ_O should be greater than a soft limit, a set-point λ_{OSetp} , which enables a tradeoff between emission, fuel consumption, and response time.
- 2) λ_O is not allowed to go below a hard minimum limit λ_{Omin} , otherwise there will be too much smoke. λ_{Omin} is always smaller than λ_{OSetp} .
- 3) x_{egr} should follow its set-point $x_{egrSetp}$. There will be more NO_x if the EGR-fraction is too low and there will be more smoke if the EGR-fraction is too high.
- 4) The engine torque, M_e , should follow the set-point M_{eSetp} from the drivers demand.
- 5) The turbocharger speed, n_t , is not allowed to exceed a maximum limit n_{tmax} , preventing turbocharger damage.
- 6) The pumping losses, M_p , should be minimized in order to decrease the fuel consumption.

The aim is now to develop a control structure that achieves all these control objectives when the set-points for EGR-fraction and engine torque are reachable.

III. DIESEL ENGINE MODEL

A diesel engine model is used to capture and give insight into the important system properties and also used in simulations for tuning and validation of the developed controller structure. The model is focused on the gas flows, see Fig. 2, and has seven states: intake and exhaust manifold pressures (p_{im} and p_{em}), oxygen mass fraction in the intake and exhaust manifold

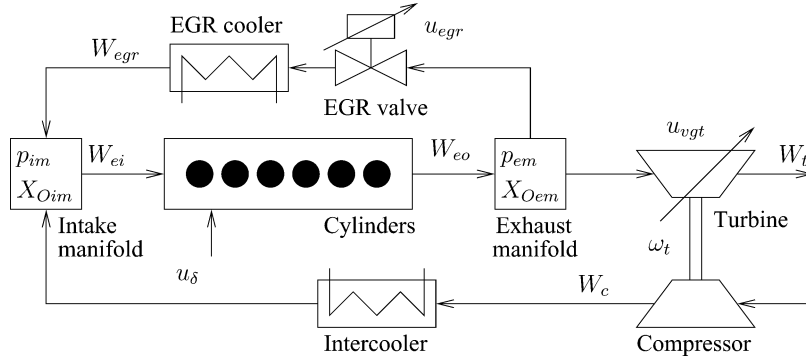


Fig. 2. Sketch of the diesel engine model used for simulation, control design, and tuning. It has five main states related to the engine (p_{im} , p_{em} , X_{Oim} , X_{Oem} , and ω_t) and two states for actuator dynamics (\tilde{u}_{egr} and \tilde{u}_{vgt}).

(X_{Oim} and X_{Oem}), turbocharger speed (ω_t), and two states describing the actuator dynamics for the two control signals (\tilde{u}_{egr} and \tilde{u}_{vgt}). These states are collected in a state vector x

$$x = (p_{im} \quad p_{em} \quad X_{Oim} \quad X_{Oem} \quad \omega_t \quad \tilde{u}_{egr} \quad \tilde{u}_{vgt})^T. \quad (1)$$

There are no state equations for the manifold temperatures. The reason is that the pressures and the turbocharger speed govern the system properties in Section IV, while the temperature states have only minor effects on these system properties.

It is important that the model can be utilized both for different vehicles having the same engine but different driveline parameters and for engine testing, calibration, and certification in an engine test cell. In many of these situations the engine operation is defined by the rotational speed n_e , for example given as a drivecycle, and therefore it is natural to parameterize the model using engine speed. The resulting model is thus expressed in state space form as

$$\dot{x} = f(x, u, n_e) \quad (2)$$

where the engine speed n_e is considered as an input to the model, and u is the control input vector

$$u = (u_\delta \quad u_{egr} \quad u_{vgt})^T \quad (3)$$

which contains mass of injected fuel u_δ , EGR-valve position u_{egr} , and VGT actuator position u_{vgt} . The EGR-valve is closed when $u_{egr} = 0\%$ and open when $u_{egr} = 100 = 0\%$. The VGT is closed when $u_{vgt} = 0\%$ and open when $u_{vgt} = 100 = 0\%$.

The model is a mean value engine model [16], and the equations are given below. A detailed description and derivation of the model is given in [17] together with a tuning methodology, a validation against test cell measurements, and a description of the nomenclature. The derivatives of the state variables are given by (4)–(7) where the right-hand sides are given by (8)–(15). The performance variables are defined by (16) and (17).

Manifolds

$$\begin{aligned} \frac{d}{dt} p_{im} &= \frac{R_a T_{im}}{V_{im}} (W_c + W_{egr} - W_{ei}) \\ \frac{d}{dt} p_{em} &= \frac{R_e T_{em}}{V_{em}} (W_{eo} - W_t - W_{egr}) \end{aligned} \quad (4)$$

$$\frac{d}{dt} X_{Oim} = \frac{R_a T_{im}}{p_{im} V_{im}} ((X_{Oem} - X_{Oim}) W_{egr} + (X_{Oc} - X_{Oim}) W_c) \quad (5)$$

$$\frac{d}{dt} X_{Oem} = \frac{R_e T_{em}}{p_{em} V_{em}} (X_{Oe} - X_{Oem}) W_{eo}. \quad (6)$$

Actuator dynamics and turbo speed

$$\begin{aligned} \frac{d}{dt} \tilde{u}_{egr} &= \frac{1}{\tau_{egr}} (u_{egr}(t - \tau_{degr}) - \tilde{u}_{egr}) \\ \frac{d}{dt} \tilde{u}_{vgt} &= \frac{1}{\tau_{vgt}} (u_{vgt} - \tilde{u}_{vgt}) \\ \frac{d}{dt} \omega_t &= \frac{P_t \eta_m - P_c}{J_t \omega_t}. \end{aligned} \quad (7)$$

Cylinder

$$W_{ei} = \frac{p_{im} n_e V_d}{120 R_a T_{im}} \eta_{vol}(p_{im}, n_e), \quad W_f = \frac{10^{-6}}{120} u_\delta n_e n_{cyl} \quad (8)$$

$$W_{eo} = W_f + W_{ei}, \quad X_{Oe} = \frac{W_{ei} X_{Oim} - W_f (O/F)_s}{W_{eo}} \quad (9)$$

$$T_{em} = T_{em} \left(\frac{p_{em}}{p_{im}}, W_f, W_{eo} \right). \quad (10)$$

EGR-valve

$$W_{egr} = \frac{A_{egr} (\tilde{u}_{egr}) p_{em} \Psi_{egr} \left(\frac{p_{im}}{p_{em}} \right)}{\sqrt{T_{em} R_e}}. \quad (11)$$

Turbine

$$\frac{W_t \sqrt{T_{em}}}{p_{em}} = A_{vgt} \max f_{\Pi_t}(\Pi_t) f_{vgt}(\tilde{u}_{vgt}), \quad \Pi_t = \frac{p_{amb}}{p_{em}} \quad (12)$$

$$P_t \eta_m = \eta_{tm}(\omega_t, T_{em}, \Pi_t) W_t c_{pe} T_{em} (1 - \Pi_t^{1-1/\gamma_e}). \quad (13)$$

Compressor

$$W_c = \frac{p_{amb} \pi R_c^3 \omega_t}{R_a T_{amb}} \Phi_c(\omega_t, \Pi_c), \quad \Pi_c = \frac{p_{im}}{p_{amb}} \quad (14)$$

$$P_c = \frac{W_c c_{pa} T_{amb}}{\eta_c (W_c, \Pi_c)} (\Pi_c^{1-1/\gamma_a} - 1). \quad (15)$$

Performance variables

$$x_{egr} = \frac{W_{egr}}{W_c + W_{egr}}, \quad \lambda_O = \frac{W_{ei} X_{Oim}}{W_f (O/F)_s}, \quad n_t = \omega_t \frac{30}{\pi} \quad (16)$$

$$M_p = \frac{V_d}{4\pi} (p_{em} - p_{im}), \quad M_e = M_{ig} - M_p - M_{fric} \quad (17)$$

$$M_{ig} = \frac{1}{4\pi} u_\delta 10^{-6} n_{cyl} q_{HV} \eta_{igch} \left(1 - \frac{1}{r_c^{\gamma_{cyl}-1}} \right) \quad (18)$$

$$M_{fric} = \frac{V_d}{4\pi} 10^5 (c_{fric1} n_e^2 + c_{fric2} n_e + c_{fric3}). \quad (19)$$

IV. SYSTEM PROPERTIES

An analysis of the behavior and characteristics of the system gives valuable insight into the control problem and is important for a successful design of the control structure (see for example [18]). An extensive system analysis has been performed and is given in [19]. The main results are summarized below and in Section IV-A the pumping losses are analyzed to give insight into how to handle objective 6 in Section II-B.

Model responses to steps in VGT position and EGR-valve show that λ_O has non-minimum phase behaviors, overshoots, and sign reversals (this is well known and shown in [18]). The fundamental physical explanation of these system properties is that the system consists of two dynamic effects that interact: a fast pressure dynamics in the manifolds and a slow turbocharger dynamics. These two dynamic effects often work against each other and change in size which results in the system properties above. The precise condition for the sign reversal is due to a complex interaction between flows, temperatures, and pressures in the entire engine [19].

Both the non-minimum phase behavior and the sign reversal in the channel $u_{vgt} \rightarrow \lambda_O$ occur in operating points where the engine frequently operates. Therefore, these two properties must be considered in the control design (this will be discussed in Section V-B). For the other channel $u_{egr} \rightarrow \lambda_O$ both the non-minimum phase behavior and the sign reversal only occur in operating points where λ_O , pumping loss M_p , and turbocharger speed n_t are high. Consequently, there are significant drawbacks when operating in these operating points. Therefore, the control structure should be designed so that these operating points are avoided (see Section V-B).

The channel $u_{egr} \rightarrow x_{egr}$ has a positive DC-gain. The channel $u_{vgt} \rightarrow x_{egr}$ has a negative DC-gain, except for a sign reversal that occur in a small operating region with low torque, low to medium engine speed, half to fully open EGR-valve, and half to fully open VGT.

Linearized diesel engine models are analyzed over the entire operating region in [19] showing that these models have a zero in the right half plane and are therefore non-minimum phase. Further, the relative gain array is analyzed for these models in [19] showing that the best input-output pairing for SISO controllers is $u_{egr} \rightarrow \lambda_O$ and $u_{vgt} \rightarrow x_{egr}$ in the regions where the engine frequently operates.

A. Pumping Losses in Steady State

A mapping of the pumping losses in steady state, is shown in Fig. 3, covering the entire operating region (at 20 different u_{vgt} points, 20 different u_{egr} points, 3 different n_e points, and 3 different u_δ points). It gives insight into how to achieve the pumping work minimization in the control structure. Fig. 3 shows that the pumping losses $p_{em} - p_{im}$ decrease with

increasing EGR-valve and VGT openings except in a small operating region with low torque, low engine speed, half to fully open EGR-valve, and half to fully open VGT, where there is a sign reversal in the gain from VGT to pumping losses. In Section V-E the resulting control behavior in this corner is discussed.

V. CONTROL STRUCTURE

The control design objective is to coordinate u_δ , u_{egr} , and u_{vgt} in order to achieve the control objectives stated in Section II-B. The diesel engine is a nonlinear and coupled system and one could consider using a multivariable nonlinear controller. However, based on the system analysis in the previous section, it is possible to build a controller structure using min/max-selectors and SISO controllers for EGR and VGT control, and to use feedforward for fuel control. As will be shown, this can be done systematically by mapping each loop in (24) and (25) to the control objectives via system analysis. The resulting structure of loops is the main result together with the rationale for it, but within the structure (24) and (25) different SISO controllers could be used. However, throughout the presentation PID controllers will be used. The foremost reasons are that all control objectives will be shown to be met and that PID controllers are widely accepted by industry.

The solution is presented step by step in the following sections, but a MATLAB/SIMULINK schematic of the full control structure is shown in Fig. 4, where all signals and the fuel controller are included together with the EGR and VGT controller depicted in Fig. 1.

A. Signals, Set-Points, and a Limit

The signals needed for the controller are assumed to be either measured or estimated using observers. The measured signals are engine speed (n_e), intake and exhaust manifold pressure (p_{im}, p_{em}), and turbocharger speed (n_t). The observed signals are the mass flow into the engine W_{ei} , oxygen mass fraction X_{Oim} , λ_O and x_{egr} . All these signals can be seen in the block "Signals" in Fig. 4.

The set-points and the limit needed for the controller (see Fig. 4) vary with operation conditions during driving. These signals are provided by an engine and emission management system as depicted in Fig. 1. The limit and the set-points are obtained from measurements and tuned to achieve stable combustion and the legislated emissions requirements. They are then represented as lookup tables being functions of operating conditions.

B. Main Feedback Loops

The starting point for the design is the structure in Fig. 1 in Section II. In the presentation to follow the resulting choice [see (20) and (21)] is presented first and then the analysis that motivates it is given. The main loops are

$$u_{egr} = -\text{PID}_1(e_{\lambda_O}) \quad (20)$$

$$u_{vgt} = -\text{PID}_3(e_{x_{egr}}) \quad (21)$$

where $e_{\lambda_O} = \lambda_{O\text{Setp}} - \lambda_O$ and $e_{x_{egr}} = x_{egr\text{Setp}} - x_{egr}$. These two main feedback loops are selected to handle items 1 and 3 of

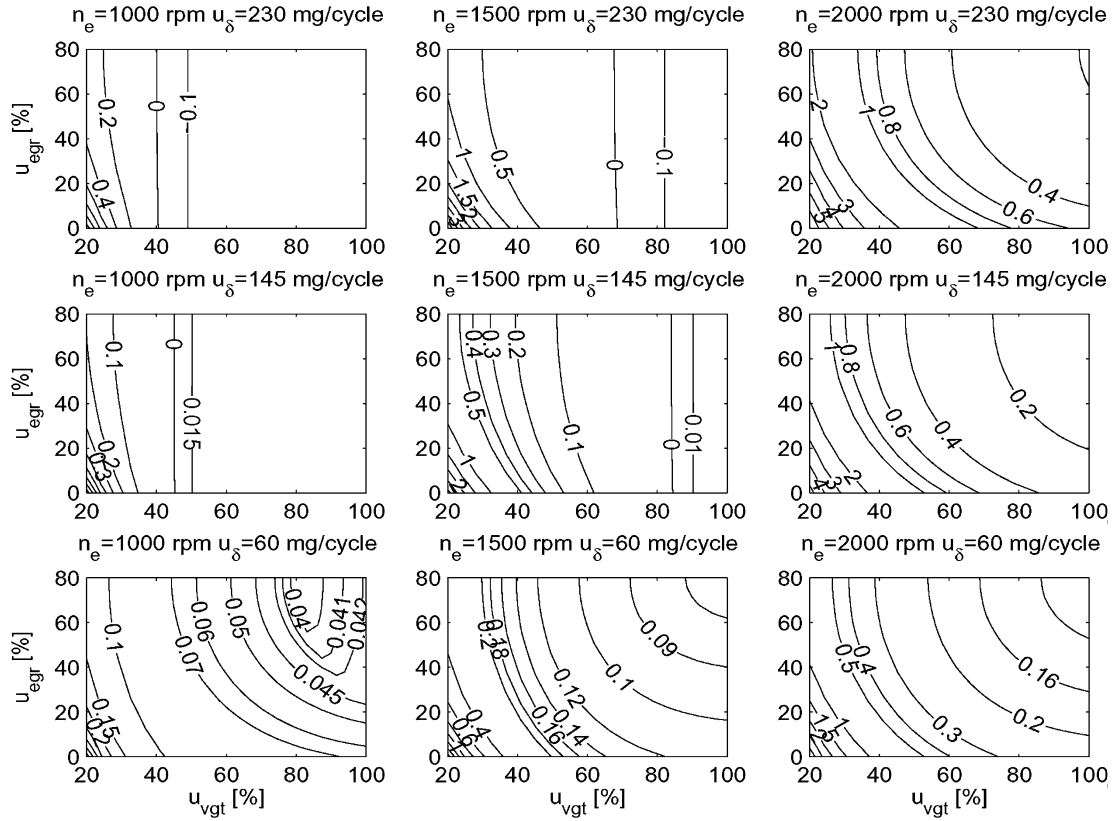


Fig. 3. Contour plots of $p_{em} - p_{im}$ [bar] in steady-state at 3 different n_e and 3 different u_δ , showing that $p_{em} - p_{im}$ decreases with increasing EGR-valve and VGT opening, except in the left bottom plot where there is a sign reversal in the gain from u_{vgt} to $p_{em} - p_{im}$.

the control objectives stated in Section II-B. In the first loop λ_O is controlled to a set-point λ_{OSetp} with the control signal u_{egr} and in the second loop intake manifold EGR-fraction, x_{egr} , is controlled to its set-point, $x_{egrSetp}$, with the control signal u_{vgt} . The PID controllers have a minus sign since the corresponding channels have negative DC-gains in almost the entire operating region (see Section IV).

The rationale behind the choice of the two main feedback loops are as follows. Relating to the system properties in Section IV, both actuators could straightforwardly be chosen for control of the EGR-fraction. However, for both actuators the λ_O performance variable requires care, and the proposed choice of main control loops relies on the following facts. First, the channel from u_{vgt} to λ_O has a sign reversal and a non-minimum phase behavior (see Section IV), that are avoided in the proposed structure (20) because u_{egr} is used to control λ_O . Second, also the channel from u_{egr} to λ_O has a sign reversal and a non-minimum phase behavior in some few operating points where the EGR-valve is closed to half open (see Section IV). However, in all these operating points λ_O is much larger than its set-point λ_{OSetp} which makes the EGR-valve to open up [according to (20)]. Consequently, the system will leave these operating points, and the influence of the non-minimum phase behavior and the sign reversal thus only have effects in transients passing these operating points.

Another reason for the choice of the main control loops are that more undershoots in λ_O will appear if the main control loops are switched. In such a case a system analysis shows that

the fast decrease in λ_O , coupled to a load increase, will cause a closing of the VGT before a closing of the EGR-valve, leading to an increase in the EGR mass flow and therefore an unnecessary decrease in λ_O in the beginning of the transient (see [20] for more details). Further, an analysis of the relative gain array supports the proposed input-output pairing for the main control loops according to Section IV.

C. Additional Feedback Loops

In order to achieve the control objectives 3 and 5 stated in Section II-B, two additional feedback loops are added to the main control loops (20) and (21). Also in this section, the equations are stated first, and then the reasons are given. Two loops are added according to

$$u_{egr} = \min(-\text{PID}_1(e_{\lambda_O}), \text{PID}_2(e_{x_{egr}})) \quad (22)$$

$$u_{vgt} = \max(-\text{PID}_3(e_{x_{egr}}), -\text{PID}_4(e_{nt})) \quad (23)$$

where $e_{nt} = n_{tSetp} - n_t$. Note that there is no minus sign for PID_2 since the corresponding channel has positive DC-gain. All other channels have negative DC-gain in almost the entire operating region (see Section IV). All the PID controllers have integral action, and $\text{PID}_4(e_{nt})$ benefits from a derivative part in order to predict high turbocharger speeds. The channel $u_{egr} \rightarrow \lambda_O$ also has a large time constant, but there is a lower demand on the bandwidth for $\text{PID}_1(e_{\lambda_O})$ compared to $\text{PID}_4(e_{nt})$, and consequently $\text{PID}_1(e_{\lambda_O})$ does not need a derivative part. None of the other PID controllers need a derivative part [20].

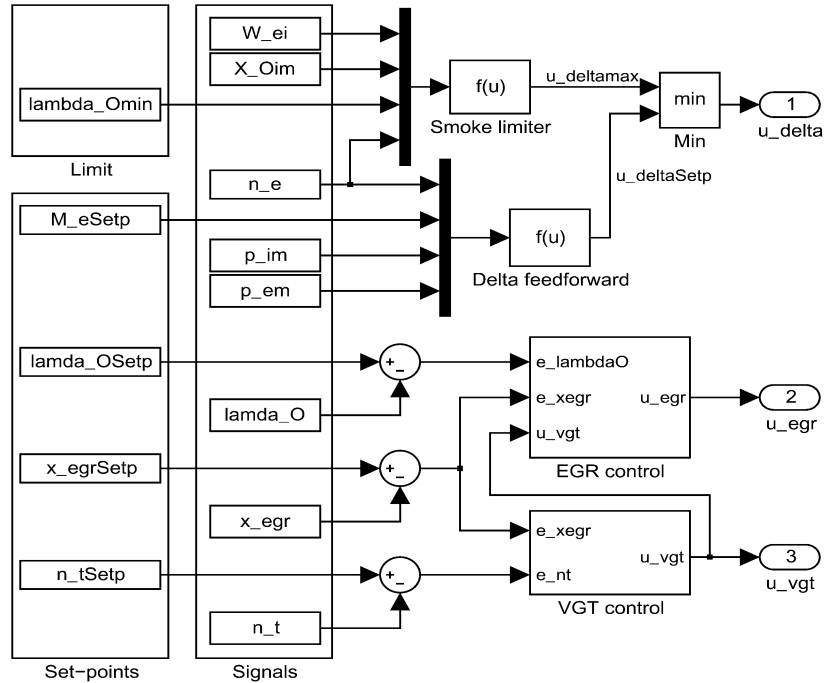


Fig. 4. Proposed control structure, as MATLAB/SIMULINK block diagram, showing; a limit, set-points, measured and observed signals, fuel control with smoke limiter, together with the controllers for EGR and VGT.

The additional feedback loops in the structure (22) and (23), are motivated as follows. In operating points with low engine torque there is too much EGR, although the VGT is fully open. To achieve control objective 3 also for these operating points, a lower EGR-fraction x_{egr} is obtainable by closing the EGR-valve u_{egr} using $PID_2(e_{xegr})$ in (22). The appropriate value for u_{egr} is then the smallest value of the outputs from the two different PID controllers, i.e., the more closed EGR setting is used. In order to get a simple control structure, $x_{egrSetp}$ is set larger than zero in operating points where $e_{\lambda_O} > 0$ and $u_{egr} = 0$ so that $PID_3(e_{xegr})$ in (23) closes the VGT in order to increase λ_O . In this specific situation, a larger $x_{egrSetp}$ gives a faster VGT closing.

To achieve control objective 5 and avoid over-speeding of the turbo, the VGT is also influenced by the turbine speed n_t in (23). In this case n_t is controlled with u_{vgt} to a set-point n_{tSetp} which has a value slightly lower than the maximum limit n_{tmax} in order to avoid that overshoots shall exceed n_{tmax} . The appropriate value for u_{vgt} is then the largest value of the outputs from the two different controllers, which means that the VGT is opened up, thereby decreasing the input torque to the turbocharger, and thereby keeping its speed within limits.

D. Minimizing Pumping Work

The control structure (22) and (23) is not guaranteed to minimize the pumping work. This can be understood from the model equations as follows. It is clear from (11) that a given flow W_{egr} can be achieved for different combinations of flow area $A_{egr}(\dot{u}_{egr})$ and $(p_{em}\Psi_{egr}(p_{im}/p_{em}))/\sqrt{T_{em}}$. The key observation is that there are many combinations of the flow area and pressure loss that can give the same flow, and consequently there are many u_{egr} and u_{vgt} that can give the same x_{egr} in cases when $\lambda_O > \lambda_{OSetp}$. Thus in some cases when $\lambda_O > \lambda_{OSetp}$ both u_{egr}

and u_{vgt} are governed by e_{xegr} . In stationary conditions, when $PID_2(e_{xegr})$ and $PID_3(e_{xegr})$ in (22) and (23) have converged, the controller fulfills the control objectives but the EGR-valve and VGT are not guaranteed to minimize the pumping work.

To achieve control objective 6, i.e., to minimize the pumping work, two additional control modes are added to the control structure (22) and (23) according to

$$u_{egr}(t_i) = \begin{cases} \min(-PID_1(e_{\lambda_O}), \\ PID_2(e_{xegr})), & \text{if } u_{vgt}(t_{i-1}) = 100 \\ -PID_1(e_{\lambda_O}), & \text{else} \end{cases} \quad (24)$$

$$u_{vgt}(t_i) = \begin{cases} 100, & \text{if } (u_{vgt}(t_{i-1}) = 100) \\ \&(e_{xegr} < 0.01) \\ \max(-PID_3(e_{xegr}), \\ -PID_4(e_{nt})), & \text{else.} \end{cases} \quad (25)$$

In this structure u_{egr} is calculated using a minimum selector only when $u_{vgt} = 100$, compared to (22) that always has a minimum selector. This subtle difference results in minimized pumping work in stationary points by striving to open the actuators as much as possible. Looking at the pumping work minimization in more detail the important controller action is coupled to λ_O , and in particular the operating conditions where there is a degree of freedom, i.e., when $\lambda_O > \lambda_{OSetp}$. For these conditions there are now two cases. In the first case the proposed controller strives to reduce λ_O by opening the EGR-valve, through the second row in (24). To maintain $x_{egrSetp}$, this action also forces the VGT to be opened as much as possible. Either λ_{OSetp} is reached or $PID_1(e_{\lambda_O})$ saturates at fully open, due to the integral action. In the other case, coupled to the first rows in (24) and (25), the VGT is fully open and it is necessary to reduce x_{egr} by closing the EGR-valve to reach $x_{egrSetp}$. In both

cases the actuators are thus opened as much as possible while achieving control objectives 1 and 3.

From the physics we know that opening a valve reduces the pressure differences over the corresponding restriction, in particular (11) results in a lower pressure loss and minimized pumping work (17). Therefore control objective 6 is achieved through the mechanism that was explained above and that opens the EGR-valve and VGT. These properties are also confirmed in Fig. 3, which shows that the lowest pumping work is achieved when the EGR-valve and VGT are opened as much as possible while keeping the control objectives. The only exceptions are in operating points with low torque, low engine speed, half to fully open EGR-valve, and half to fully open VGT. In these operating points there is a sign reversal in the gain from VGT to pumping work. However, the proposed control structure is not extended to handle this sign reversal, since the maximum profit according to simulations would only be 2.5 mBar, which is an insignificant value.

In case 1 in (25) the VGT is locked to fully open (the value 100) until $e_{x_{egr}} > 0.01$ in order to avoid oscillations between case 1 and 2 in (24).

Simulations have been performed, under the same conditions as in [21], and they show that the proposed control structure (24) and (25) reduces the pumping work with 66% compared to the control structure (22) and (23). However, when considering the modeling and measurements errors the reduction is calculated to be at least 56%, and this leads to a reduction in fuel consumption with 4%.

E. Effect of Sign Reversal in VGT to EGR-Fraction

The system properties in Section IV show that the DC-gain from u_{vgt} to x_{egr} has a sign reversal in a small operating region, and an important question is what effect this sign reversal has on the control performance. This sign reversal occurs in operating points with half to fully open EGR-valve and half to fully open VGT and in these operating points λ_O is much larger than its set-point λ_{OSetp} which makes the EGR-valve to be fully open if $u_{vgt} < 100$ [according to case 2 in (24)]. If $u_{vgt} < 100$ and $x_{egr} < x_{egrSetp}$ in the beginning of a transient the VGT position decreases until $x_{egr} = x_{egrSetp}$ (according to $PID_3(e_{x_{egr}})$ in (25)), consequently, the system will leave the operating region with reversed sign. If $u_{vgt} < 100$ and $x_{egr} > x_{egrSetp}$ in the beginning of a transient the VGT position increases until it is fully open and then $PID_2(e_{x_{egr}})$ in (24) becomes active and closes the EGR-valve until $x_{egr} = x_{egrSetp}$. Consequently, the system can not get caught in the operating region with reversed sign while $PID_3(e_{x_{egr}})$ in (25) is active, i.e., the system can not get caught in an unstable mode. However, the effect of this sign reversal is that there exist two sets of solutions for the EGR-valve and the VGT-position for the same value of $x_{egrSetp}$ depending on if $x_{egr} < x_{egrSetp}$ or if $x_{egr} > x_{egrSetp}$ in the beginning of a transient. However, the proposed control structure is not extended to handle this sign reversal, since the maximum profit in pumping work would only be 2.5 mBar, which is the same value as the maximum profit in the previous section due to that the sign reversal in VGT to EGR-fraction occurs partly in the same operating points as the sign reversal in VGT to pumping work.

F. Feedforward Fuel Control

Engine torque control, control objective 4, is achieved by feedforward from the set-point M_{eSetp} by utilizing the torque model and calculating the set-point value for u_δ according to

$$u_{\delta Setp} = c_1 M_{eSetp} + c_2 (p_{em} - p_{im}) + c_3 n_e^2 + c_4 n_e + c_5$$

which is obtained by solving u_δ from (17)–(19). This control is implemented in the block “Delta feedforward” in Fig. 4.

Aggressive transients can cause λ_O to go below its hard limit λ_{Omin} resulting in exhaust smoke. The PID controller in the main loop (20) is not designed to handle this problem. To handle control objective 2, a smoke limiter is used which calculates the maximum value of u_δ . The calculation is based on engine speed n_e , mass flow into the engine W_{ei} , oxygen mass fraction X_{Oim} and lower limit of oxygen/fuel ratio λ_{Omin}

$$u_{\delta max} = \frac{W_{ei} X_{Oim} 120}{\lambda_{Omin} (O/F)_s 10^{-6} n_{cy1} n_e}$$

implemented in the block “Smoke limiter” in Fig. 4.

Combining these two the final fuel control command is

$$u_\delta = \min(u_{\delta max}, u_{\delta Setp}) \quad (26)$$

which concludes the description and the motivation of the control structure in Fig. 4.

VI. AUTOMATIC CONTROLLER TUNING

In the proposed structure there are four PID controllers that need tuning. There are conflicting goals as it is not possible to get both good transient response and good EGR tracking at the same time so tradeoffs have to be made. This can be a cumbersome work and therefore an efficient and systematic method has been developed. As a result the following nonlinear least squares problem is formulated

$$\min V(\theta) \text{ s.t. } \theta > 0 \quad (27)$$

where θ is the parameter vector

$$\theta = [K_1, T_{i1}, K_2, T_{i2}, K_3, T_{i3}, K_4, T_{i4}, T_{d4}]^T \quad (28)$$

where K_j , T_{ij} , and T_{dj} are the control parameters for the PID controllers that have the following parameterization:

$$PID_j(e) = K_j \left(e + \frac{1}{T_{ij}} \int e dt + T_{dj} \frac{de}{dt} \right) \quad (29)$$

where the index j is the number of the different PID controllers in (24) and (25). The PID controllers are implemented in incremental form which leads to anti-windup and bump-less transfer between the different control modes [22].

The control objectives in Section II-B and the system properties in Section IV are mapped to a quadratic performance mea-

measure, where each term reflects either control objectives or actuator stress. The motivation for each term is given below, and the cost function is calculated as

$$\begin{aligned}
 V(\theta) = & \sum_{i=1}^N \gamma_{Me} \left(\frac{e_{Me}(t_i)}{M_{eNorm}} \right)^2 + \gamma_{egr} \left(\frac{e_{xegr}(t_i)}{x_{egrNorm}} \right)^2 \\
 & + \left(\frac{u_{egr}(t_i) - u_{egr}(t_{i-1})}{u_{egrNorm}} \right)^2 \\
 & + \left(\frac{u_{vgt}(t_i) - u_{vgt}(t_{i-1})}{u_{vgtNorm}} \right)^2 \\
 & + \gamma_{nt} \left(\frac{\max(n_t(t_i) - n_{tmax}, 0)}{n_{tNorm}} \right)^2 \quad (30)
 \end{aligned}$$

where t_i is the time at sample number i . All terms in (30) are normalized to get the same order of magnitude for the five terms, and this means that the weighting factors have an order of magnitude as $\gamma_{Me} \approx 1$ and $\gamma_{egr} \approx 1$.

These terms have been derived by analyzing the control objectives and system properties, and the connections and motives for them are given in the following paragraphs. Objectives 2 and 6 are fulfilled directly as they are built into the structure in terms of the smoke limiter and the pumping work minimization presented in Section V.

Term 1: This term is the most intricate one and it is coupled to objectives 1 and 4 and they are in their turn related to each other through the system properties. They are related since a good transient response, especially during tip-in maneuvers, is connected to availability of oxygen and thus a fast λ_O -controller will give good transient response.

A further motivation for choosing to minimize engine torque deficiency, $e_{Me} = M_{eSetp} - M_e$ comes from the fact that negative values of $e_{\lambda_O} = \lambda_{OSetp} - \lambda_O$ are allowed, and it is positive e_{λ_O} values that have to be decreased. Now noting that torque deficiency occurs when the smoke limiter in Section V-F restricts the amount of fuel injected, i.e., when $\lambda_O = \lambda_{Omin}$ (see Fig. 5 between 309 and 313 s). Since $\lambda_{Omin} < \lambda_{OSetp}$ a positive e_{λ_O} exists when torque deficiency occurs.

One could also consider using e_{λ_O} directly but such a choice is not sufficiently sensitive during transients where there is a need for air. Due to the smoke limiter, e_{λ_O} will be limited to the difference $\lambda_{OSetp} - \lambda_{Omin}$ when the smoke limiter is active and this does not reflect the actual demand for air and λ_O during transients. Thus the torque deficiency is selected as performance measure.

Term 2: This term is directly coupled to objective 3 and strives to minimize the EGR error ($e_{xegr} = x_{egrSetp} - x_{egr}$).

Terms 3 and 4: These terms are coupled to the general issue of avoiding actuator stress, e.g., oscillatory behavior in the EGR valve or in the VGT control signals. The terms have equal weight since the control signals are of the same magnitude.

Term 5: This term is a direct consequence of objective 5 and avoids that the turbocharger speed exceeds its maximum limit. A high penalty is used, $\gamma_{nt} \approx 10^3$, to capture that this is a safety critical control loop.

To solve (27), a transient selection method and a solver for the optimization problem has been developed in [23]. As a result

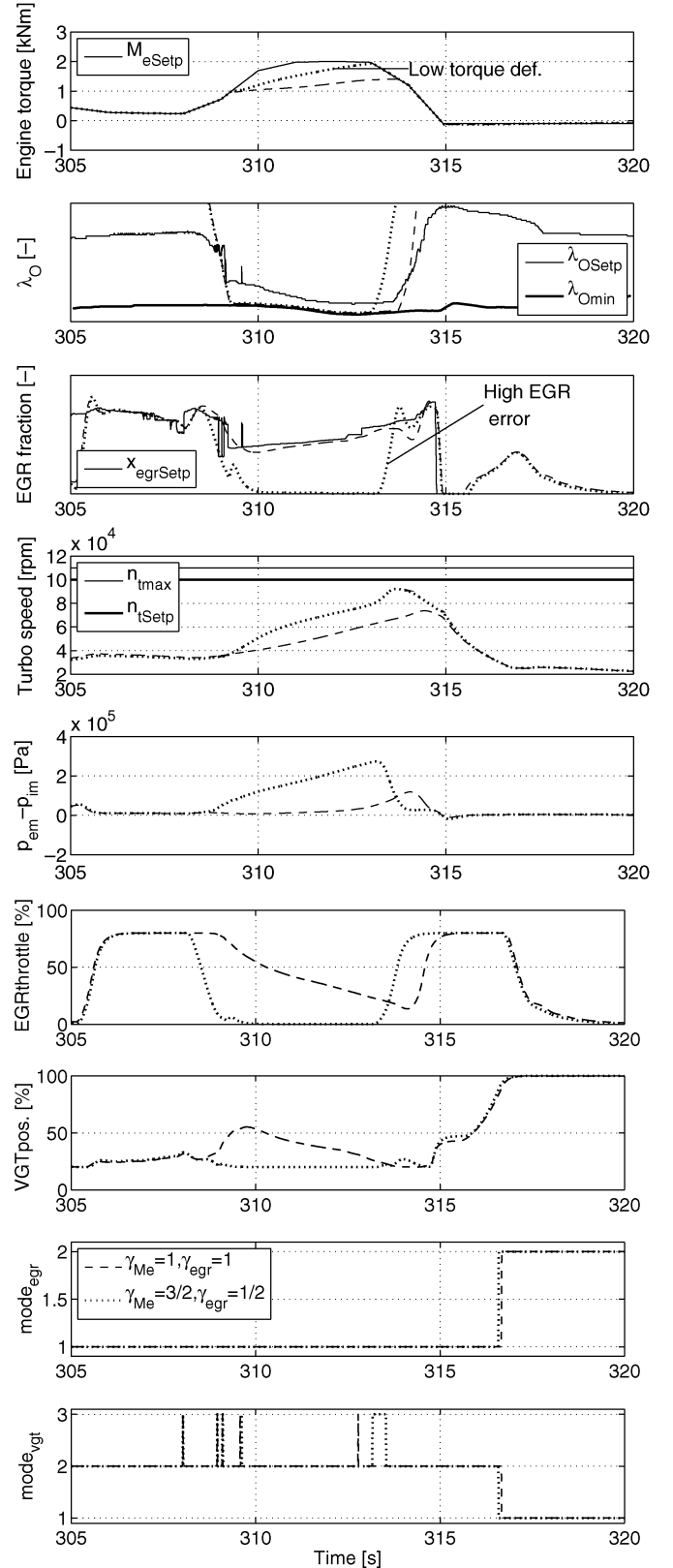


Fig. 5. Comparison between two simulations of the control system using two sets of weighting factors. The first set is $\gamma_{Me} = 1$ and $\gamma_{egr} = 1$ and the second set is $\gamma_{Me} = 3/2$ and $\gamma_{egr} = 1/2$. The latter set of weighting factors gives less torque deficiency but more EGR error and more pumping losses compared to the first set of weighting factors.

computational time is reduced from 30 to 3 hours when using only the selected transients instead of a full ETC cycle.

In summary all control objectives are considered and handled in the tuning. Furthermore, the difficulty of tuning of the individual controllers, related to the tradeoff between transient response (λ_O) and EGR errors, is efficiently handled by the two weighting factors γ_{Me} and γ_{egr} , as illustrated in Section VII-A.

VII. EUROPEAN TRANSIENT CYCLE SIMULATIONS

The control tuning method is illustrated and applied, and a simulation study is performed on the European Transient Cycle (ETC). The cycle consists of three parts representing different driving conditions: urban (0–600 s), rural (600–1200 s), and highway (1200–1800 s) driving.

The closed-loop system, consisting of the model in Section III and the proposed control structure in Section V (depicted in Fig. 4), is simulated in MATLAB/SIMULINK. The set points for λ_O and x_{egr} are authentic recordings that have been provided by industry. A remark is that an observer is not used in the simulations. Instead a low pass filter, with the time constant 0.02 s, is used to model the observer dynamics for all variables assumed to come from an observer. This is done in the block “Signals” in Fig. 4. The different signals in the cost function (30) are calculated by simulating the complete system and sampling the signals with a frequency of 100 Hz.

A. Balancing Control Objectives

The weighting factors γ_{Me} , γ_{egr} , and γ_{nt} in the cost function (30) are tuning parameters. When tuning these, tradeoffs are made between torque deficiency, EGR error, pumping losses, and turbo over-speed.

A tuning strategy for the relation between γ_{Me} and γ_{egr} is to increase γ_{Me} when a controller tuner wants to decrease the torque deficiency and increase γ_{egr} when a controller tuner wants to decrease the EGR error and the pumping losses. It is important that the sum $\gamma_{Me} + \gamma_{egr}$ is constant in order to avoid influence of the third and fourth term in the cost function when tuning the first and the second term. In the following section, $\gamma_{Me} + \gamma_{egr} = 2$. A tuning strategy for avoiding turbo over-speeding is to increase γ_{nt} until the fifth term becomes equal to zero.

Illustration of Performance Tradeoffs: The tradeoffs between torque deficiency, EGR error, and pumping losses are illustrated in Fig. 5, where the control system is simulated on an aggressive transient from the ETC cycle with two sets of weighting factors. The first set is $\gamma_{Me} = 1$ and $\gamma_{egr} = 1$ and the second set is $\gamma_{Me} = 3/2$ and $\gamma_{egr} = 1/2$. The latter set of weighting factors punishes the torque deficiency more than the first one. Fig. 5 also shows the control modes for the EGR valve

$$\text{mode}_{egr} = \begin{cases} 1, & \text{if PID}_1(e_{\lambda_O}) \text{ active} \\ 2, & \text{if PID}_2(e_{x_{egr}}) \text{ active} \end{cases} \quad (31)$$

and the VGT position

$$\text{mode}_{vgt} = \begin{cases} 1, & \text{if } u_{vgt} = 100 \\ 2, & \text{if PID}_3(e_{x_{egr}}) \text{ active} \\ 3, & \text{if PID}_4(e_{nt}) \text{ active.} \end{cases} \quad (32)$$

The setting $\gamma_{Me} = 3/2$ and $\gamma_{egr} = 1/2$ gives less torque deficiency but more EGR error and more pumping losses compared to $\gamma_{Me} = 1$ and $\gamma_{egr} = 1$, which is seen in Fig. 5 in

the following way. Between 305 and 308 s the engine torque is low which leads to a high λ_O , an open EGR-valve, and that the VGT position controls the EGR-fraction so that the EGR error is low. Thereafter, an increase in engine torque at 308 s leads to a decrease in λ_O and therefore a closing of the EGR-valve. This closing is faster if γ_{Me}/γ_{egr} is increased from 1 to 3 which leads to a lower EGR-fraction (i.e., more EGR error), a more closed VGT position, a faster increase in turbocharger speed, and consequently a lower torque deficiency. Note that the torque deficiency and the EGR error can not be low at the same time during the aggressive transient. Note also that there are more pumping losses at $\gamma_{Me} = 3/2$ and $\gamma_{egr} = 1/2$ due to that the EGR-valve and the VGT position are more closed. Consequently, in dynamic conditions trade-offs are made between torque deficiency and pumping loss. However, it is important to note that the pumping loss is still minimized in stationary points by the proposed control structure in both cases in Fig. 5 compared to the other control structure in Section V-C that gives higher pumping losses.

All the tradeoffs between different performance variables described in this section are also valid for the complete cycle. This is illustrated by simulating the complete ETC cycle [20].

VIII. ENGINE TEST CELL EXPERIMENTS

The control structure proposed in Section V (depicted in Fig. 4) is applied and validated in an engine test cell on the complete ETC cycle. The goal is to experimentally verify that the control structure achieves the control objectives stated in Section II-B and to compare it to the current production control system.

An available production observer, similar to the one in [11], is used to estimate the oxygen mass fraction X_{Oim} . Once X_{Oim} is estimated, the mass flow into the engine W_{ei} , λ_O , and x_{egr} are calculated using (8) and (16). The engine speed (n_e), intake and exhaust manifold pressure (p_{im}, p_{em}) and turbocharger speed (n_t) are measured with production sensors. The set points for λ_O and x_{egr} are given as functions of the operating point and have been provided by industry and are the same for all controllers. The injection timing control has been provided by industry. The PID parameters are initially tuned using the method in Section VI with $\gamma_{Me} = 3/2$ and $\gamma_{egr} = 1/2$, and are then manually fine tuned in the engine test cell experiments. The motive for choosing these weighting factors is that they represent a worst case scenario concerning the EGR-error and the pumping work. This worst case scenario is used in the experiments in order to show that the proposed control system reduces the pumping work compared to the current production control system for all reasonable sets of weighting factors. This can be understood as follows. According to Fig. 5, the selected weighting factors $\gamma_{Me} = 3/2$ and $\gamma_{egr} = 1/2$ give low torque deficiency, high pumping work, and high EGR-errors and consequently NO_x emissions that perhaps do not fulfill the legislated emission limits. The pumping work becomes higher when increasing γ_{Me}/γ_{egr} , however this leads to even higher EGR-errors and increases the NO_x emissions which is undesirable. Therefore, $\gamma_{Me} = 3/2$ and $\gamma_{egr} = 1/2$ are considered to be a worst case scenario concerning the EGR-error and the pumping work.

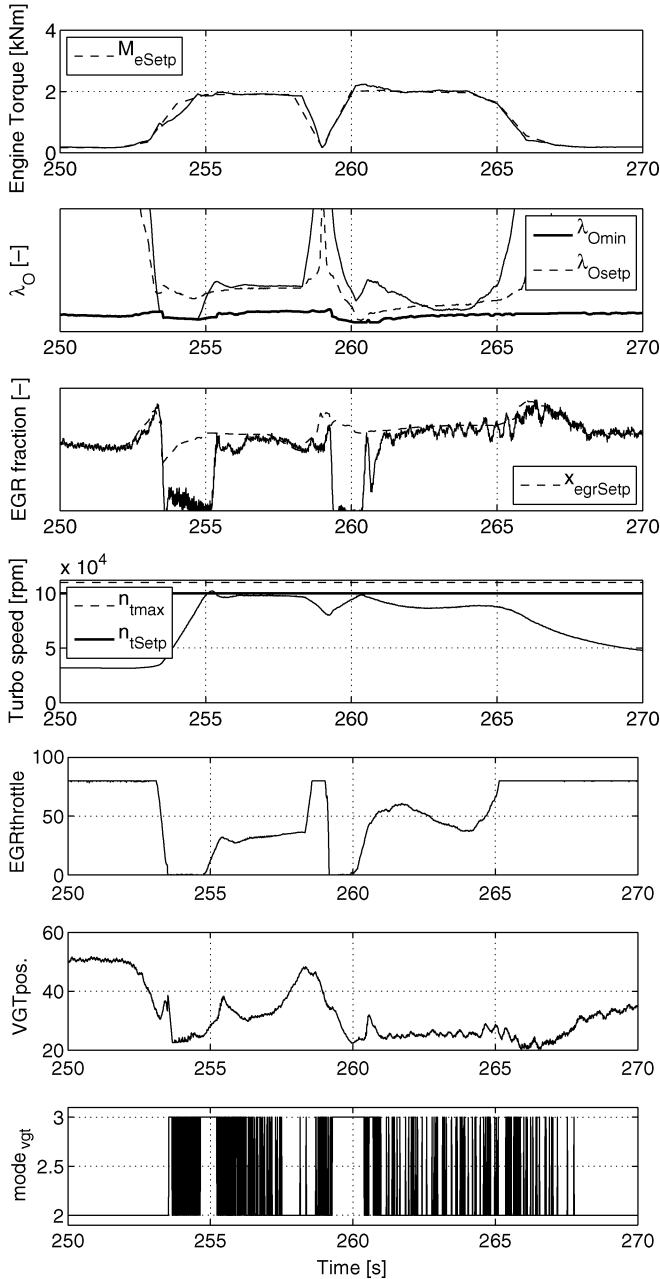


Fig. 6. Validation of the proposed control structure in an engine test cell on an aggressive transient from the ETC cycle. Note that this transient was not used in the automatic tuning process in Section VI. The proposed control structure achieves all the control objectives stated in Section II-B. The signal $mode_{egr}$ is equal to one for this transient.

A. Investigation of the Control Objectives

The validation of the control structure on the complete ETC cycle shows that it achieves the control objectives in Section II-B. This is illustrated by showing an aggressive transient from the ETC cycle in Fig. 6. Note that this transient was not used in the automatic tuning process in Section VI. The fulfillment is assessed in the following way.

Control objective 1 is achieved since λ_O is larger than the set-point λ_{OSetp} except when the torque increases rapidly at 253 s and when λ_O has a small undershoot at 263 s. To handle this,

the controller closes both the EGR-throttle and the VGT-position at 253 s and the controller closes the EGR-throttle at 263 s in order to increase λ_O as fast as possible. Control objective 2 is achieved since λ_O is always larger than or equal to the minimum limit λ_{Omin} . Note that the smoke limiter is active when $\lambda_O = \lambda_{Omin}$. Control objective 3 is achieved since x_{egr} follows its set-point $x_{egrSetp}$ except when $\lambda_O = \lambda_{Omin}$ at 253.5 s and when λ_O decreases rapidly at 259 s. At these points it is important to increase λ_O , so therefore the EGR-throttle is closed which results in an EGR-error. Control objective 4 is achieved since M_e follows its set-point M_{eSetp} except when the smoke limiter is active at 253.5 s. Control objective 5 is achieved since the turbocharger speed is always smaller than its maximum value n_{tmax} . Finally, control objective 6 is achieved since the EGR-throttle is opened as much as possible when $\lambda_O > \lambda_{OSetp}$, yielding minimized pumping loss. This can be seen at 250, 258.5, and 265 s where the EGR-throttle is fully open while the VGT controls the EGR-fraction. Quantitatively, following the calculation in Section V-D, the pumping losses are calculated to be reduced at least 50%. The oscillations in $mode_{vgt}$ are due to measurement noise and that the outputs from $PID_3(e_{x_{egr}})$ and $PID_4(e_{nt})$ have approximately the same values at these points. These oscillations are not harmful, since the PID controllers are implemented in incremental form yielding bump-less transfer.

Consequently, the proposed control structure achieves all the control objectives in Section II-B. Further, the experiment shows that the control structure has good control performance with fast control of the performance variables and systematic handling of tradeoffs.

B. Comparison to the Current Production Control System

The proposed control structure is compared to a current production system on the complete ETC cycle by comparing λ_O -error $E_{\lambda_O} = \sum_{i=1}^N \max(e_{\lambda_O}(t_i), 0)$, x_{egr} -error $E_{x_{egr}} = \sum_{i=1}^N |e_{x_{egr}}(t_i)|$, and pumping losses $PMEP = \sum_{i=1}^N (p_{em}(t_i) - p_{im}(t_i))$ where t_i is the time at sample number i . The comparison in Table I shows that the two controllers have approximately the same control performance in the main performance variables λ_O and x_{egr} and that the production controller has 26% higher pumping losses yielding 1.4% higher fuel consumption, that is significant for a truck engine. The differences in E_{λ_O} and $E_{x_{egr}}$ between the controllers are only due to that the tuning of the controllers have different tradeoffs between λ_O -error and x_{egr} -error. The tuning of the proposed controller is selected to be a worst case scenario concerning the EGR-error and the pumping work according to Section VIII. Since the production controller gives more pumping losses for this worst case scenario, it will have at least 26% higher pumping losses for all reasonable sets of weighting factors in the tuning of the proposed controller.

IX. CONCLUSION

A control structure with PID controllers and selectors has been proposed and investigated for coordinated control of oxygen/fuel ratio λ_O and intake manifold EGR-fraction x_{egr} . These were chosen both as performance and feedback variables

TABLE I
MEASURES E_{λ_O} , $E_{x_{egr}}$, AND $PMEP$ FOR TWO DIFFERENT CONTROLLERS
OVER THE ETC CYCLE, SHOWING THAT THE PRODUCTION CONTROLLER HAS
26% HIGHER PUMPING LOSSES. THE MEASURES ARE NORMALIZED WITH
RESPECT TO THE PROPOSED CONTROLLER

Controller	E_{λ_O}	$E_{x_{egr}}$	$PMEP$
Proposed controller	1.00	1.00	1.00
Production controller	1.50	0.60	1.26

since they give information about when it is allowed to minimize the pumping work. This pumping work minimization is a novel and simple strategy and compared to another control structure which closes the EGR-valve and the VGT more, the pumping work is substantially reduced. Further, the chosen variables are strongly coupled to the emissions and therefore they give advantages in an industrial perspective where the inner loop is combined with an outer loop in an engine management system in a way suited for efficient calibration.

Based on a system analysis, λ_O is controlled by the EGR-valve and x_{egr} by the VGT-position, mainly to handle the sign reversal from VGT to λ_O . Besides controlling the two main performance variables, λ_O and x_{egr} , the control structure also successfully handles torque control, including torque limitation due to smoke control, and supervisory control of turbo charger speed for avoiding over-speeding. Further, the systematic analysis of the control problem in Section IV was used to map the control objectives to the controller structure, and this conceptual coupling to objectives gives the foundation for systematic tuning, be it manual or automatic. This was utilized to develop an automatic controller tuning method. The objectives to minimize pumping work and ensure the minimum limit of λ_O are handled by the structure, while the other control objectives are captured in a cost function, and the tuning is formulated as a nonlinear least squares problem.

Different performance tradeoffs are necessary and they were illustrated on the ETC. The proposed controller is validated in an engine test cell, where it is experimentally demonstrated that the controller achieves all control objectives and that the current production controller has at least 26% higher pumping losses compared to the proposed controller.

ACKNOWLEDGMENT

The authors would like to thank M. Jennische, D. Elfvik, D. Vestgöte, and Y. Strand for their support with the experiments at Scania.

REFERENCES

[1] J. Heywood, *Internal Combustion Engine Fundamentals*. New York: McGraw-Hill, 1988.
 [2] L. Guzzella and A. Amstutz, "Control of diesel engines," *IEEE Control Syst. Mag.*, vol. 18, no. 5, pp. 53–71, Oct. 1998.
 [3] M. Jankovic, M. Jankovic, and I. Kolmanovsky, "Constructive lyapunov control design for turbocharged diesel engines," *IEEE Trans. Control Syst. Technol.*, vol. 8, no. 2, pp. 288–299, Mar. 2000.

[4] M. Nieuwstadt, I. Kolmanovsky, P. Moraal, A. Stefanopoulou, and M. Jankovic, "EGR-VGT control schemes: Experimental comparison for a high-speed diesel engine," *IEEE Control Syst. Mag.*, vol. 20, no. 3, pp. 63–79, Jun. 2000.
 [5] J. Rückert, A. Schloßer, H. Rake, B. Kinoo, M. Krüger, and S. Pischinger, "Model based boost pressure and exhaust gas recirculation rate control for a diesel engine with variable turbine geometry," presented at the IFAC Workshop: Adv. Autom. Control, Karlsruhe, Germany, 2001.
 [6] M. Ammann, N. Fekete, L. Guzzella, and A. Glattfelder, "Model-based control of the VGT and EGR in a turbocharged common-rail diesel engine: Theory and passenger car implementation," SAE, Warrendale, PA, Tech. Paper 2003-01-0357, Jan. 2003.
 [7] A. Amstutz and L. D. Re, "EGO sensor based robust output control of EGR in diesel engines," *IEEE Trans. Control System Technology*, pp. 37–48, 1995.
 [8] J. Chauvin, G. Corde, N. Petit, and P. Rouchon, "Motion planning for experimental airpath control of a diesel homogeneous charge-compression ignition engine," *Control Eng. Pract.*, vol. 16, pp. 1081–1091, 2008.
 [9] M. Jung, K. Glover, and U. Christen, "Comparison of uncertainty parameterisations for H-infinity robust control of turbocharged diesel engines," *Control Eng. Pract.*, vol. 13, pp. 15–25, 2005.
 [10] M. Nieuwstadt, P. Moraal, I. Kolmanovsky, A. Stefanopoulou, P. Wood, and M. Widdle, "Decentralized and multivariable designs for EGR-VGT control of a diesel engine," presented at the IFAC Workshop, Adv. Autom. Control, OH, 1998.
 [11] R. Rajamani, "Control of a variable-geometry turbocharged and wastegated diesel engine," in *Proc. 1 MECH E Part D J. Autom. Eng.*, Nov. 2005, pp. 1361–1368.
 [12] A. Stefanopoulou, I. Kolmanovsky, and J. Freudenberg, "Control of variable geometry turbocharged diesel engines for reduced emissions," *IEEE Trans. Control Syst. Technol.*, vol. 8, no. 4, pp. 733–745, Jul. 2000.
 [13] K. Zhou, J. C. Doyle, and K. Glover, *Robust and Optimal Control*. Upper Saddle River, NJ: Prentice-Hall, 1996.
 [14] S. Nakayama, T. Fukuma, A. Matsunaga, T. Miyake, and T. Wakimoto, "A new dynamic combustion control method based on charge oxygen concentration for diesel engines," SAE World Congr., Warrendale, PA, Tech. Paper 2003-01-3181, 2003.
 [15] J. Rückert, F. Richert, A. Schloßer, D. Abel, O. Herrmann, S. Pischinger, and A. Pfeifer, "A model based predictive attempt to control boost pressure and EGR-rate in a heavy duty diesel engine," presented at the IFAC Symp. Adv. Autom. Control, Salerno, Italy, 2004.
 [16] U. Kiencke and L. Nielsen, *Automotive Control Systems for Engine, Driveline, and Vehicle*, 2nd ed. New York: Springer-Verlag, 2005.
 [17] J. Wahlström and L. Eriksson, "Modeling of a diesel engine with VGT and EGR including oxygen mass fraction," Linköping Univ., Linköping, Sweden, 2006.
 [18] I. Kolmanovsky, A. Stefanopoulou, P. Moraal, and M. van Nieuwstadt, "Issues in modeling and control of intake flow in variable geometry turbocharged engines," presented at the 18th IFIP Conf. Syst. Model. Opt., Detroit, MI, Jul. 1997.
 [19] J. Wahlström, "Control of EGR and VGT for emission control and pumping work minimization in diesel engines," Ph.D. dissertation, Dept. Elect. Eng., Linköping Univ., Linköping, Sweden, 2009.
 [20] J. Wahlström, "Control of EGR and VGT for emission control and pumping work minimization in diesel engines," Licentiate Thesis, Dept. Elect. Eng., Linköping Univ., Linköping, 2006.
 [21] J. Wahlström, L. Eriksson, L. Nielsen, and M. Pettersson, "PID controllers and their tuning for EGR and VGT control in diesel engines," presented at the Preprints 16th IFAC World Congr., Prague, Czech Republic, 2005.
 [22] K. J. Åström and T. Hägglund, *PID Controllers: Theory, Design and Tuning*, 2nd ed. Research Triangle Park, PA: Instrument Society of America, 1995.
 [23] J. Wahlström, L. Eriksson, and L. Nielsen, "Controller tuning based on transient selection and optimization for a diesel engine with EGR and VGT," SAE World Congr., Detroit, MI, 2008-01-0985, 2008.